N-24
167905
34

NASA Contractor Report 191142

An Analytical/Numerical Correlation Study of the Multiple Concentric Cylinder Model for the Thermoplastic Response of Metal Matrix Composites

Marek-Jerzy Pindera, Robert S. Salzar, and Todd O. Williams
University of Virginia
Charlottesville, Virginia

Prepared for
Lewis Research Center
Under Contract NAS3–26571

National Aeronautics and Space Administration

(NASA-CR-191142) AN ANALYTICAL/NUMERICAL CORRELATION STUDY OF THE MULTIPLE CONCENTRIC CYLINDER MODEL FOR THE THERMOPLASTIC RESPONSE OF METAL MATRIX COMPOSITES Final Report (Virginia Univ.) 34 p

N93-27086

Unclas

G3/24 0167905

AN ANALYTICAL/NUMERICAL CORRELATION STUDY OF THE MULTIPLE CONCENTRIC CYLINDER MODEL FOR THE THERMOPLASTIC RESPONSE OF METAL MATRIX COMPOSITES

by

Marek-Jerzy Pindera
Robert S. Salzar
Todd O. Williams

University of Virginia
Charlottesville, Virginia 22903

ABSTRACT

The utility of a recently developed analytical micromechanics model for the response of metal matrix composites under thermal loading is illustrated by comparison with the results generated using the finite-element approach. The model is based on the concentric cylinder assemblage consisting of an arbitrary number of elastic or elastoplastic sublayers with isotropic or orthotropic, temperature-dependent properties. The elastoplastic boundary-value problem of an arbitrarily layered concentric cylinder is solved using the local/global stiffness matrix formulation (originally developed for elastic layered media) and Mendelson's iterative technique of successive elastic solutions. These features of the model facilitate efficient investigation of the effects of various microstructural details, such as functionally graded architectures of interfacial layers, on the evolution of residual stresses during cool down. The available closed-form expressions for the field variables can readily be incorporated into an optimization algorithm in order to efficiently identify optimal configurations of graded interfaces for given applications. Comparison of residual stress distributions after cool down generated using finite-element analysis and the present micromechanics model for four composite systems with substantially different temperature-dependent elastic, plastic and thermal properties illustrates the efficacy of the developed analytical scheme.

INTRODUCTION

The concentric cylinder geometry has been employed quite frequently during the past thirty years for modeling the response of unidirectional composites. The early models are based on a single fiber embedded in a cylindrical shell (Hashin, 1962; Hill, 1965; Mulhern and Rogers, 1967; Dvorak and Rao, 1976a,b). These models have been used to predict elastic moduli or their bounds for general, three-dimensional loading, as well as thermoelastic and inelastic response under axisymmetric loading. More recently, generalizations of these models have been proposed in order to include the interaction of the composite cylinder with the surrounding medium (Dvorak and Bahei-El-Din, 1979; Christensen and Lo, 1979), or to take into account the effect of

microstructural details on the overall composite response (Hashin, 1990; Benveniste et al., 1991; Sutcu, 1992; Warwick and Clyne, 1991). The microstructural details include the presence of carbon coating around certain types of fibers, the layered morphology of such ceramic fibers as the SCS6 SiC fiber used in titanium matrix composites, as well as the presence of an interface or interphase layer between the fiber and the matrix. The interfacial region can arise naturally due to chemical reaction between the fiber and the matrix (Wawner and Gundel, 1991), or can be introduced deliberately in order to minimize residual fabrication stresses (Arnold et al., 1990). With the exception of the model proposed by Sutcu which deals with elastic response of unidirectional metal matrix composites with layered SiC fibers, the aforementioned models focus on specific geometries involving only a few concentric cylinders.

Recently, an analytical elastoplastic solution to the micromechanics concentric cylinder model under axisymmetric thermal loading that allows consideration of **arbitrarily** layered configurations has been constructed by Pindera et al. (1992). The solution is based on the **local/global stiffness matrix formulation** originally developed by Bufler (1971) for stress analysis of isotropic, elastic layered media, and Mendelson's **method of successive elastic solutions** for elastoplastic problems with Prandtl-Reuss constituents (Mendelson, 1983). Applications of the local/global stiffness matrix technique to the elastic stress analysis problems of composite materials and structures have been presented by Pindera (1991). Derstine and Pindera (1988) used the method to develop an approximate solution to the problem of an arbitrarily laminated composite tube under axisymmetric loading with inelastic graphite/epoxy plies that were modeled using the endochronic theory.

In the local/global stiffness matrix formulation, the solution of a given boundary-value problem is reformulated in terms of the interfacial displacements as the basic unknowns in place of the eigenvectors associated with the eigenfunctions that satisfy the governing differential equations for the given problem. This reformulation entails construction of a local stiffness matrix that relates the tractions at the outer boundaries of a layer to the corresponding interfacial displacements. By assembling the local stiffness matrices along the main diagonal of the global stiffness matrix in an overlapping fashion, the interfacial continuity conditions and the external boundary conditions are identically satisfied. In elastoplastic problems, the local stiffness matrix equation that describes the response of a layer, and thus the global stiffness matrix for the entire assemblage, involves integrals of plastic strain distributions in the individual layers. These integrals appear as vectors on the right hand side of the system of equations that ensures satisfaction of boundary conditions and continuity of interfacial tractions and displacements. Since these integrals depend implicitly on the unknown interfacial displacements, the system of equations must be solved in an iterative fashion. The solution developed by Pindera et al. (1992) utilizes

the classical incremental plasticity model for the inelastic response of the matrix phase in an unidirectional metal matrix composite, and employs Mendelson's method of successive elastic solutions to solve the system of nonlinear equations.

The reformulation of the boundary-value problem in terms of the interfacial displacements as the basic unknowns using the local/global stiffness matrix approach offers a number of advantages over the standard formulation. First of all, the construction of the global stiffness matrix can be automated very easily, facilitating addition of extra layers without any difficulty. This construction also eliminates certain redundant equations that arise from the application of interfacial continuity and boundary condition equations in the standard formulation, resulting in nearly 50% reduction in the size of the system of simultaneous equations for a large number of layers. Furthermore, as the elements of the stiffness matrices for different types of elastic (isotropic, transversely isotropic, orthotropic) and inelastic (isotropic) layers have been provided in closed form, a given boundary-value problem does not have to be resolved each time a particular concentric cylinder assemblage is considered. Different configurations are efficiently handled by assembling the global stiffness matrix in an appropriate fashion using the provided local stiffness matrices.

The elastoplastic solution of the multiple concentric cylinder (MCC) under axisymmetric thermal loading based on the local/global stiffness matrix formulation is very well suited for computer implementation, facilitating efficient parametric studies for developing new composite materials with elastoplastic constituents. Since the solution methodology is analytical rather than numerical (eg. finite-element or finite-difference schemes), there is no need to generate meshes or grids every time the geometrical details of the concentric cylinder are changed. Different configurations are conveniently handled by changing a few lines in the input file of a computer program that can be executed on a personal computer/work station. It is this feature that makes computer implementation of the solution very attractive for use by the materials scientist, designer and analyst alike. The construction of the input data file is simple and can be further facilitated by a user-friendly interface that allows the user to specify the input parameters in an interactive fashion through menu-driven data entry.

The ability to easily vary the number and arrangement of the concentric cylinders makes this method ideal for a wide variety of applications involving axisymmetric loading of advanced unidirectional composites. These applications include the reduction of residual stresses in metal matrix composites using single or multiple compliant/compensating interfacial layers as suggested by Arnold and co-workers (1990, 1992) (see also Jansson and Leckie (1992)), and design of engineered interfaces for improved performance (Arnold and Wilt, 1992). Further, since the solution is analytic, with expressions for the various field quantities provided in closed form, it

can readily be incorporated into an optimization algorithm in order to efficiently identify optimal interfacial layer configurations or morphologies for given applications. The method also facilitates efficient discretization of functionally graded composites into an arbitrarily large number of layers in order to model spatial property variations as accurately as is desired. Thus either discretely-graded or continuously-graded interfacial regions can be investigated.

Thus far, the MCC model has been employed to investigate the effect of: 1.) morphology of SCS6 SiC fibers; 2.) architecture of interfacial layers; and 3.) microstructure of the $\alpha_2 + \beta$ titanium aluminide matrix, on the evolution of residual stresses in SiC/Ti_3Al unidirectional composites (Pindera et al., 1992; Pindera and Freed, 1992). A recent investigation addresses the effectiveness of graded interfacial layers in reducing residual stresses in titanium matrix composites subjected to both monotonic and cyclic thermal loading (Williams et al., 1993). An investigation addressing the problem of optimization of residual stresses in metal matrix composites using multiple layers at the fiber/matrix interface is currently in progress.

A limited comparison between the predictions of the MCC model and the finite-element results generated using a commercially available code was presented by Pindera et al. (1992) for the problem of a composite cylinder with a single interfacial layer subjected to a temperature drop. The purpose of this paper is to present an extensive comparison between the predictions of the MCC model and the finite-element results obtained with the commercially-available code ABAQUS (1989) for several concentric cylinder configurations with single and multiple interfacial layers, and different constituents, subjected to thermal loading. The ultimate objective is to demonstrate the utility of the developed analytical solution methodology for efficiently and accurately investigating the thermoplastic response of MMC's under axisymmetric thermal loading in the presence of various microstructural details.

ANALYTICAL MODEL

The analytical model is based on a long, cylindrical assemblage of an arbitrary number of concentric cylinders or shells perfectly bonded to each other, Figure 1. Each of the cylindrical shells is either elastic or inelastic. The elastic shells may be isotropic, transversely isotropic, or orthotropic (radially or circumferentially), while the inelastic shells are taken as initially isotropic and are modelled using the time-independent incremental plasticity with isotropic hardening. All the material parameters governing the response of the elastic and inelastic layers are functions of temperature. The geometrical model is thus general enough to allow one to model the actual morphologies of fiber, interfacial layer and matrix phases in sufficient detail.

A distribution of displacements and stresses in the individual phases of the concentric composite cylinder model is sought under the conditions of a spatially uniform temperature change

that varies with time. A solution to the outlined elastoplastic boundary-value problem is obtained using the displacement formulation. In solving the boundary-value problem, the following notation is adopted. The inner solid core is denoted by a subscript or superscript 1 and the outermost cylindrical shell by n. The inner radius of the kth shell is denoted by r_{k-1} and the outer radius by r_k. The traction and displacement components at the inner and outer radii of the kth shell are assigned superscripts "-" and "+", respectively.

For the prescribed axisymmetric loading, the longitudinal, tangential and radial displacement components u, v and w, referred to the cylindrical coordinate system x–r–θ centered at the origin of the concentric cylinder assemblage have the form,

$$\begin{aligned} u &= u(x) = \varepsilon_0 \, x \\ w &= w(r) \\ v &= 0 \end{aligned} \tag{1}$$

where ε_0 is the same uniform longitudinal strain for all layers. These displacement components yield the following strain components in the cylindrical coordinate system,

$$\varepsilon_{xx} = \frac{du}{dx} = \varepsilon_0 \, , \quad \varepsilon_{\theta\theta} = \frac{w(r)}{r} \, , \quad \varepsilon_{rr} = \frac{dw(r)}{dr} \tag{2}$$

with the shear strain components identically zero. Since the strain components are either constant or functions of only the radial coordinate r, the stress components are at most functions of r, and therefore the stress equilibrium equations in cylindrical coordinates reduce to the single equation,

$$\frac{d\sigma_{rr}}{dr} + \frac{\sigma_{rr} - \sigma_{\theta\theta}}{r} = 0 \tag{3}$$

The governing differential equation for the radial displacement w(r) in each shell is obtained by expressing the stress components σ_{rr} and $\sigma_{\theta\theta}$ in Equation (3) in terms of w(r) and its gradient using stress-strain equations and strain-displacement relations given by Equation (2). For problems in cylindrical coordinates, the stress-strain equations for an orthotropic material in the presence of thermal loading and inelastic effects, and in the absence of shear strains, are given by,

$$\begin{Bmatrix}\sigma_{xx}\\ \sigma_{\theta\theta}\\ \sigma_{rr}\end{Bmatrix}=\begin{bmatrix}C_{xx} & C_{x\theta} & C_{xr}\\ C_{x\theta} & C_{\theta\theta} & C_{\theta r}\\ C_{xr} & C_{\theta r} & C_{rr}\end{bmatrix}\begin{Bmatrix}\varepsilon_{xx}-\varepsilon_{xx}^{in}-\alpha_{xx}(T-T_0)\\ \varepsilon_{\theta\theta}-\varepsilon_{\theta\theta}^{in}-\alpha_{\theta\theta}(T-T_0)\\ \varepsilon_{rr}-\varepsilon_{rr}^{in}-\alpha_{rr}(T-T_0)\end{Bmatrix} \tag{4}$$

In the above, ε_{xx}, $\varepsilon_{\theta\theta}$, ε_{rr} are total strains, ε_{xx}^{in}, $\varepsilon_{\theta\theta}^{in}$, ε_{rr}^{in} are inelastic strains, and $\alpha_{xx}(T-T_0)$, $\alpha_{\theta\theta}(T-T_0)$, $\alpha_{rr}(T-T_0)$ are thermal strains, with T_0 denoting a reference temperature and T denoting the current temperature. The corresponding constitutive equations for an isotropic or transversely isotropic material can be obtained by equating the appropriate stiffness matrix elements.

Given the functional form of the displacement field, the strain-displacement equations and the constitutive equations in a cylindrical shell, the governing differential equation for the radial displacement w(r) in each shell is obtained from the surviving equilibrium equation in the form,

Transversely isotropic, elastic layers ($C_{x\theta}=C_{xr}$, $C_{\theta\theta}=C_{rr}$, $\alpha_{\theta\theta}=\alpha_{rr}$)

$$\frac{d^2w}{dr^2}+\frac{1}{r}\frac{dw}{dr}-\frac{w}{r^2}=0 \tag{5a}$$

Orthotropic, elastic layers

$$\frac{d^2w}{dr^2}+\frac{1}{r}\frac{dw}{dr}-\frac{1}{r^2}\frac{C_{\theta\theta}}{C_{rr}}w=\frac{1}{r}\left[\frac{(C_{\theta x}-C_{xr})}{C_{rr}}\varepsilon_0+\sum_{i=x,\theta,r}\frac{(C_{ri}-C_{\theta i})}{C_{rr}}\alpha_{ii}(T-T_0)\right] \tag{5b}$$

Isotropic, inelastic layers

$$\frac{d^2w}{dr^2}+\frac{1}{r}\frac{dw}{dr}-\frac{1}{r^2}w=\frac{1}{r}\sum_{i=x,\theta,r}\frac{(C_{ri}-C_{\theta i})}{C_{rr}}\varepsilon_{ii}^{in}(r)+\frac{d}{dr}\sum_{i=x,\theta,r}\frac{C_{ri}}{C_{rr}}\varepsilon_{ii}^{in}(r) \tag{5c}$$

where the distribution of the inelastic strains, $\varepsilon_{ii}^{in}(r)$, is assumed to be known at the beginning of each thermal load increment.

The solution of the above equations is obtained subject to the external boundary condition, $\sigma_{rr}(r_n) = 0$, the interfacial displacement and traction continuity conditions, $w_{k-1}(r_{k-1}) = w_k(r_{k-1})$, $\sigma_{rr}^{k-1}(r_{k-1}) = \sigma_{rr}^{k}(r_{k-1})$, and the longitudinal equilibrium condition, $\int_{A_c} \sigma_{xx} dA_c = 0$, where A_c is the cross-sectional area of the concentric cylinder assemblage.

Using standard techniques, solutions to the governing differential equations are obtained in the form,

Transversely isotropic, elastic layers

$$w(r) = A_1 r + \frac{A_2}{r} \tag{6a}$$

Orthotropic, elastic layers

$$w(r) = A_1 r^{\lambda} + A_2 r^{-\lambda} + \frac{(C_{\theta x} - C_{rx})}{(C_{rr} - C_{\theta\theta})} r\varepsilon_0 + \sum_{i=x,\theta,r} \frac{(C_{ri} - C_{\theta i})}{(C_{rr} - C_{\theta\theta})} \alpha_{ii} r(T - T_0) \tag{6b}$$

Isotropic, inelastic layers

$$w(r) = \frac{1}{2r} \int_{r_{k-1}}^{r} \sum_{i=x,\theta,r} \frac{(C_{ri} + C_{\theta i})}{C_{rr}} \varepsilon_{ii}^{in}(r') r' dr' + \frac{r}{2} \int_{r_{k-1}}^{r} \sum_{i=x,\theta,r} \frac{(C_{ri} - C_{\theta i})}{C_{rr}} \varepsilon_{ii}^{in}(r') \frac{dr'}{r'} + \tag{6c}$$

$$A_1 r + \frac{A_2}{r} + \frac{1}{2} \sum_{i=x,\theta,r} \frac{C_{ri}}{C_{rr}} \varepsilon_{ii}^{in}(r_{k-1}) r \left(\frac{r_{k-1}^2}{r^2} - 1\right)$$

where $\lambda = \left(\frac{C_{\theta\theta}}{C_{rr}}\right)^{1/2}$ and $r_{k-1} \le r \le r_k$.

The above solutions contain unknown coefficients A_1^k and A_2^k for each layer, as well as the unknown, uniform axial strain ε_0. For the solid core, the constant A_2^1 vanishes since the radial displacement at the center has to vanish. These unknown coefficients are determined from the boundary condition, interfacial traction and displacement continuity conditions, and the longitudinal force equilibrium condition. Application of these conditions yields a system of equations in the unknown A_1^k and A_2^k coefficients and the uniform longitudinal strain ε_0, that is solved

iteratively when the inelastic strains are present. An iterative procedure is required because the inelastic strains depend implicitly on the coefficients A_1^k and A_2^k.

In order to automate the construction of this system of equations so that any arbitrarily layered configuration can easily be considered, we reformulate the problem in terms of the interfacial radial displacements as the basic unknowns in place of the coefficients A_1^k and A_2^k by using the concept of a **local stiffness matrix**. The local stiffness matrix relates the interfacial tractions at the inner and outer radii of the kth layer to the corresponding interfacial radial displacements, and is obtained from the solutions to Equations (5a-c) (i.e. Equations (6a-c)) in conjunction with the constitutive equations and strain-displacement equations. To construct the local stiffness matrix for the kth layer, we first express the coefficients A_1^k and A_2^k in terms of the interfacial displacements $w_k(r_{k-1})$ and $w_k(r_k)$ by evaluating the solution for the radial displacement component w(r) at the appropriate locations. These expressions are then used in the equation for the radial stress component in the kth layer given in terms of the determined radial displacement field. The final step entails an evaluation of the radial stress in the kth layer at the inner and outer radii in order to generate the radial tractions at those locations.

The form of the local stiffness matrix equation for the kth layer in the state of generalized plane strain and in the presence of thermal and inelastic effects is

$$\begin{Bmatrix} -\sigma_{rr}^- \\ \sigma_{rr}^+ \end{Bmatrix}^k = \begin{bmatrix} k_{11} & k_{12} \\ k_{21} & k_{22} \end{bmatrix}^k \begin{Bmatrix} w^- \\ w^+ \end{Bmatrix}_k + \begin{Bmatrix} k_{13} \\ k_{23} \end{Bmatrix}^k \varepsilon_0 + \begin{Bmatrix} f_1 \\ f_2 \end{Bmatrix}^k (T - T_0) + \begin{Bmatrix} g_1 \\ g_2 \end{Bmatrix}^k \tag{7}$$

The elements $k_{11}^k, \ldots, k_{23}^k$ of the local stiffness matrix are functions of the geometry and elastic material properties of the kth layer (which may vary with temperature). The thermal effects are represented by f_1^k and f_2^k, which are functions of the thermal expansion coefficients for the kth layer. The plastic effects are represented by g_1^k and g_2^k, which are given in terms of the integrals of the plastic strain distribution in the given layer. The elements of the local stiffness matrix and the elements of the force vectors appearing in Equation (7) have been provided by Pindera et al. (1992) for transversely isotropic and orthotropic, elastic layers, and isotropic, inelastic layers.

Imposition of continuity of displacements and tractions along the common interfaces, together with the boundary condition on the radial stress at r_n, and the longitudinal equlibrium condition, gives rise to a system of equations in the unknown interfacial displacements expressed in the matrix form below. The first n equations result from the imposition of interfacial continuity and boundary conditions, whereas the nth+1 equation ensures that the longitudinal equilibrium is satisfied at any cross-section along the cylinder's axis.

$$\begin{bmatrix} k_{22}^1 + k_{11}^2 & k_{12}^2 & 0 & . & k_{23}^1 + k_{13}^2 \\ k_{21}^2 & k_{22}^2 + k_{11}^3 & . & . & . \\ 0 & k_{21}^3 & . & . & . \\ . & . & . & k_{22}^n & k_{23}^n \\ \phi_{22}^1 + \phi_{11}^2 & . & . & \phi_{22}^n & \sum\psi_k \end{bmatrix} \begin{Bmatrix} w_1 \\ w_2 \\ . \\ w_n \\ \varepsilon_0 \end{Bmatrix} = - \begin{Bmatrix} f_2^1 + f_1^2 \\ . \\ . \\ f_2^n \\ \sum\Omega_k \end{Bmatrix} (T - T_0) - \begin{Bmatrix} g_2^1 + g_1^2 \\ . \\ . \\ g_2^n \\ \sum\Pi_k \end{Bmatrix} \tag{8}$$

The elements of the last row, ϕ_{11}^k, ϕ_{22}^k, ψ_k, Ω_k, and Π_k have also been provided by Pindera et al. (1992). We observe that the global stiffness matrix is constructed by first superposing the local stiffness matrices along the main diagonal in an overlapping fashion, and then adding a column and a row to account for the thermal effects and the longitudinal equilibrium condition in the case of free thermal expansion/contraction. Under the conditions of plane strain, ε_0 vanishes and the nth+1 row and column are not added into the global stiffness matrix. It is a simple matter to construct a computer algorithm for assembling the global stiffness matrix.

SOLUTION PROCEDURE

The system of equations given by Equation (8) is solved iteratively at each temperature step for the specified loading after the manner suggested by Mendelson (1983). The iteration is performed on the plastic force vector that consists of the elements g_1^k, g_2^k and $\sum\Pi_k$. The elements g_1^k and g_2^k are expressed in terms of the integrals of the plastic strain distributions in the given layer that have the form (see Pindera et al. (1992)),

$$\int_{r_{k-1}}^{r_k} \sum_{i=x,\theta,r} \frac{(C_{ri} + C_{\theta i})}{C_{rr}} \varepsilon_{ii}^{in}(r') r' dr' \quad , \quad \int_{r_{k-1}}^{r_k} \sum_{i=x,\theta,r} \frac{(C_{ri} - C_{\theta i})}{C_{rr}} \varepsilon_{ii}^{in}(r') \frac{dr'}{r'} \tag{9a}$$

whereas the element Π_k has the form,

$$\int_{r_{k-1}}^{r_k} \sum_{i=x,\theta,r} C_{xi} \varepsilon_{ii}^{in}(r') r' dr' \tag{9b}$$

Since the elements of the global stiffness matrix at a given temperature are constant, only one inversion of the matrix for each sequence of iterations is required. As the elements f_1^k, f_2^k and $\sum\Omega_k$ of the thermal force vector are also constant at a given temperature, most of the

computational effort lies in evaluating the integrals in Equation (9) at each iteration. The algorithm for the iterative procedure is given in the sequel.

For the given temperature increment, the plastic strain distribution in each layer is expressed in terms of the distribution at the preceding temperature plus an increment that results from the imposed temperature change.

$$\varepsilon_{ij}^{p}(r)\,|_{\text{current}} = \varepsilon_{ij}^{p}(r)\,|_{\text{previous}} + d\varepsilon_{ij}^{p}(r) \tag{10}$$

The plastic strain increment is derived from the von Mises yield condition which, in the presence of temperature-dependent elastoplastic properties of the matrix phase, has the form

$$F = \frac{1}{2}\sigma'_{ij}\sigma'_{ij} - \frac{1}{3}\bar{\sigma}^{2}(\bar{\varepsilon}^{p}, T) = 0 \tag{11}$$

where $\bar{\sigma}$ is the effective yield stress, which is a function of both the effective plastic strain $\bar{\varepsilon}^{p}$ and temperature. The plastic strain increment is thus,

$$d\varepsilon_{ij}^{p} = \frac{\partial F}{\partial \sigma'_{ij}} d\lambda = \sigma'_{ij} d\lambda \tag{12}$$

where the proportionality constant $d\lambda$ is obtained from the consistency condition for plastic loading in the form

$$d\lambda = \frac{\sigma'_{ij} D_{ijkl}(d\varepsilon_{kl} - d\varepsilon_{kl}^{th}) + (\sigma'_{ij} C'_{ij} - \frac{2}{3}\bar{\sigma}\frac{\partial \bar{\sigma}}{\partial T})dT}{\frac{4}{9}\bar{\sigma}^{2}\frac{\partial \bar{\sigma}}{\partial \bar{\varepsilon}^{p}} + \sigma'_{ij} D_{ijkl} \sigma'_{kl}} \tag{13}$$

where $d\lambda \geq 0$ for plastic loading, $d\lambda \leq 0$ for neutral loading or unloading, and $d\varepsilon_{ij}^{th}$ are the thermal strain increments given by,

$$d\varepsilon_{ij}^{th} = [\alpha_{ij}(T) + \frac{\partial \alpha_{ij}(T)}{\partial T}(T - T_0)]dT \tag{14}$$

D_{ijkl} are the elastic stiffness elements, and $C'_{ij} = \frac{\partial D_{ijkl}}{\partial T}\varepsilon^e_{kl}$. In the present investigation, the elastoplastic stress-strain response of the matrix is taken to be bilinear so that the slope of the effective stress-plastic strain curve, $\frac{\partial \bar{\sigma}}{\partial \bar{\varepsilon}_p}$, is constant at a given temperature. Since the incremental theory of plasticity is used to calculate the plastic strain increment at each point along the radial coordinate, the inelastic analysis is valid for both loading and unloading in the plastic phases.

The plastic strain distribution in each layer is determined by calculating the plastic strains at twenty-one stations after updating the plastic strains at these locations using Equation (10). The current values for the plastic strains at these stations are then used in determining the integrals given in Equation (9), and thus the elements of the plastic force vector in Equation (8). Updated values of the interfacial displacements are then obtained from Equation (8). With a knowledge of the interfacial displacements and the axial strain ε_0, the coefficients A_1^k and A_2^k in each layer can be obtained, producing solutions for the radial displacement $w_k(r)$ from which radial and tangential total and plastic strains, and the corresponding stresses, can be obtained. These are then used to obtain new approximations for the plastic strain increments. The iterative process is terminated when the differences between two successive sets of plastic strain increments are less than some prescribed value. The above procedure is described in detail by Mendelson (1983).

NUMERICAL RESULTS AND DISCUSSION

In order to demonstrate the accuracy, efficiency and efficacy of the outlined solution technique, we investigate the evolution of residual stresses in unidirectional metal matrix composites with and without interfacial layers for four material systems with different temperature dependence of the constituents' behavior. The predictions of the MCC model subsequently are compared with the results generated using the commercially available finite-element code ABAQUS.

The considered material systems are state-of-the-art metal matrix composites under consideration for advanced aerospace applications. The four material systems chosen for the correlation study are: SiC/Ti_3Al, Al_2O_3/NiAl, Al_2O_3/NiCrAlY1, and Al_2O_3/NiCrAlY2. The properties of the indvidual constituents for these composites are listed in Table 1 (SCS6 fiber and Ti-24Al-11Nb matrix) and Table 2 (Al_2O_3 fiber and NiAl, NiCrAlY1, and NiCrAlY2 matrices). For the SiC/Ti_3Al system, residual stresses were calculated for cool down from 1500°F to 75°F. In the case of the remaining material systems, residual stresses were calculated for cool down from 2300°F to 70°F.

For the SiC/Ti_3Al system, three configurations were considered, namely; a fiber embedded in a homogeneous matrix, a fiber embedded in a matrix with a one-layer interface, and a fiber embedded in a matrix with a three-layer interface. In all cases, the outer radius of the composite cylinder was normalized to 1.0, with the normalized fiber radius of 0.6320 producing a fiber volume fraction of 0.40. For the configurations involving one- and three-layer interfaces, the outer radius of the interfacial region was 0.6952, resulting in an interfacial volume fraction of 0.08. The mechanical properties of the interface layers (with the exception of the Poisson's ratio) were taken to be one half of the matrix properties at each temperature. The thermal expansion coefficient of the single interfacial layer configuration was two times that of the matrix, while in the case of the three-layer interface configuration the thermal expansion coefficient was two, two and one half, and three times that of the matrix phase starting from the innermost layer. For the Al_2O_3 fiber systems, only one configuration was considered, namely; a fiber embedded in a matrix without an interface having the same geometry as the corresponding SiC/Ti_3Al composite.

The MCC calculations were performed using temperature increments of - 1.0°F. Convergence of plastic strain increments at the various radial locations typically did not require more than six iterations at each temperature increment. As an additional check, values of the effective stress calculated from the effective stress-plastic strain curve at various radial locations were compared with values of the effective stress based on the obtained stress components at these locations. Typically, differences were a fraction of a percent.

For the finite-element calculations, three quarter-symmetry meshes were constructed that consisted of triangular (CGPE8) and quadrilateral (CGPE10), generalized plane strain elements, Figure 2. The coarse mesh (Figure 2a) consisted of 88 elements, the medium mesh (Figure 2b) consisted of 296 elements, and the fine mesh (Figure 2c) consisted of 580 elements. Each of the three meshes has provision for inclusion of a single interfacial layer with four elements across the thickness of the interfacial region. These meshes were used to study the convergence and accuracy of the finite-element results and to compare the CPU times with the corresponding run times for the MCC calculations. Selected comparison of the axial, circumferential and radial stress components and the radial displacement at several radial locations in the fiber, interfacial layer and matrix obtained with the present analytical solution and the finite-element solution is presented in Table 3 for the SiC/Ti_3Al material system with one-layer interface. The results indicate that even with the coarse mesh the differences between the MMC and finite-element results are quite small. The fine mesh provides better approximation of the external zero-traction boundary condition and in some cases better satisfaction of the interfacial continuity conditions. For this reason, it was used to generate the remainder of the results for the SiC/Ti_3Al system with

one-layer interface, as well as for the configuration without an interface. The same mesh was also used to generate results for the Al_2O_3 fiber systems. For the SiC/Ti_3Al system with a three-layer interface, a new mesh was constructed with 708 elements that was based on the fine, 580-element mesh, Figure 3. This was done by subdividing the interfacial region into three layers while maintaining four elements through the thickness of each of the three layers. Table 4 presents a comparison of CPU times for the cool down of the SiC/Ti_3Al composite with one-layer and three-layer interfaces from 1500°F to 75°F simulated with the four finite-element meshes and the MCC model. The calculation were performed on an IBM RS-6000 machine. The efficiency of the MCC model is clearly evident.

It should be noted that the comparison of the CPU times presented above is perhaps misleading because the analytical model is one-dimensional, whereas the finite-element calculations were performed using a two-dimensional model. It would certainly have been more appropriate to generate the finite-element results using axisymmetric, generalized plane strain (line) elements. Such elements, however, are presently not available in the existing ABAQUS code. Nevertheless, the comparison presented above does give an indication of the model's efficiency. Further, while the finely-refined meshes used in the present investigation are probably not necessary for most applications, and may even be considered an "overkill", the authors nevertheless are of the opinion that in order to meet the intended objectives of this investigation, such refinement was desirable. This is because the outlined analytical solution is, in principle, an exact solution that satisfies, in addition to the field equations, all the external boundary conditions and internal continuity conditions provided that the integration of the plastic strain distributions is performed accurately. In the present case, the interfacial region was subdivided into three layers of equal thickness and the matrix phase into six, and the plastic strain distributions were calculated at twenty-one points within each layer as previously mentioned. The accuracy with which the integrals of the plastic strain distributions given in Equation (9) were calculated in generating the analytical solution, therefore, was quite high. Consequently, in order to obtain a comparable level of resolution with the finite-element approach and thus to render the comparison between the two solutions meaningful, the finely-refined mesh configuration was chosen.

SiC/Ti_3Al system

Figure 4a-c presents the axial, circumferential and radial stress distributions, respectively, in the SiC/Ti_3Al unidirectional composite without an interface, at four temperatures between the stress-free temperature of 1500°F and the final cool-down temperature of 75°F. The analytical predictions are indicated by the solid lines whereas the finite-element results are given by

different symbols superposed on the solid lines corresponding to the four different temperatures. The stress distributions at 875°F are elastic, characterized by piecewise uniform values of the axial stress throughout the entire region, and inversely quadratic dependence of the circumferential and radial stresses in the matrix phase. These baseline distributions can be compared with the distributions at the remaining temperatures which exhibit significant influence of plasticity at the fiber/matrix interface as discussed by Arnold et al. (1990). Comparing the distributions at the different temperatures allows one to delineate the elastic-plastic boundaries in the matrix phase. Clearly, the correlation between the analytical solution to the MCC model and the finite-element results is excellent.

The three stress distributions for the SiC/Ti_3Al composite with a one-layer and three-layer interface at 75°F after cool down from 1500°F are compared in Figure 5a-c. Again, the correlation between the analytical solution to the MCC model and the finite-element results for the two configurations is unquestionably excellent. Comparing the stress distributions for the one-layer and three-layer interface configurations one observes the effect of grading the thermal expansion coefficient in the interfacial region on the stress fields in the matrix phase as well as the interfacial region itself. The use of compensating layers in reducing fabrication-induced residual stresses in unidirectional metal matrix composites in the presence of matrix plasticity has been discussed by Arnold et al. (1990, 1992), as well as Pindera et al. (1992), and is currently the subject of continuing investigation.

Al_2O_3 based systems

Figure 6a-c presents the distributions of the axial, circumferential and radial stresses at 70°F after cool down from 2300°F for the three Al_2O_3 fiber-based material systems. The two NiCrAlY matrices, designated by numbers 1 and 2, differ only in the temperature dependence of the Young's moduli and yield stresses. The Young's modulus of the NiCrAlY1 matrix is between 38% and 55% higher than that of NiCrAlY2 in almost the entire temperature range (with the exception of 2400°F), while the range in which the yield stress of NiCrAlY1 exceeds that of NiCrAlY2 varies between 25% and 155%. Comparing the thermoelastoplastic properties of the NiAl matrix on the one hand, and the two NiCrAlY matrices on the other, one observes: initially similar magnitudes in the thermal expansion coefficient but a steeper rise with increasing temperature for the NiCrAlY matrices; similar magnitudes of the Young's modulus in the lower temperature range for the NiAl and NiCrAlY matrices, but a greater decline with increasing temperature for the NiCrAlY matrix; significantly lower yield stress in the NiAl matrix up to 1800°F; and the hardening slope of the NiAl matrix that is five times greater than that of the two NiCrAlY matrices.

The results in Figure 6a-c indicate that the NiCrAlY1 matrix composite produces the highest axial, circumferential and radial residual stresses, followed by the NiCrAlY2 matrix composite and then finally the NiAl matrix composite. The differences in the three residual stress distributions between the two NiCrAlY matrix composites and the NiAl matrix composite are significant. The stress distributions in the three material systems exhibit significant plasticity effects, with the NiAl matrix system showing the most uniform profiles in the matrix region. This is not surprising in view of the low values of yield stress in comparison to the yield stress of the two NiCrAlY matrices. Comparing the analytical solution of the MCC model and the finite-element results, one again observes excellent correlation.

CONCLUSIONS

The extensive comparison between the results of the analytical micromechanics model based on the multiple concentric cylinder geometry and the finite-element analysis for several different material systems exhibiting different temperature dependence of the constituents' properties and different configurations, clearly demonstrates the accuracy and the power of the developed analytical approach for modeling thermoplastic response of unidirectional metal matrix composites under axisymmetric loading. The pronounced plasticity effects observed in the response of advanced metal matrix composites currently under development for elevated temperature applications necessarily require incorporation of inelastic constitutive models for the matrix and/or fiber phases into the micromechanical stress analysis. Numerical procedures such as the finite-element or finite-difference analyses are approximate, geometry-specific and often require large computation times. The current method is an extension of the local/global stiffness matrix formulation originally developed for stress analysis of layered, elastic media, to axisymmetric elastoplastic problems and utilizes Mendelson's method of successive elastic solutions. The major advantage offered by the outlined method is the ease with which different geometric configurations involving arbitrarily layered concentric cylinders are handled. Since the method is analytic, this is easily accomplished by changing a few lines in the input data file of a computer code. This, in turn, facilitates efficient parametric studies in the course of developing new composite materials, as well as in investigating the effects of various microstructural details on the local and global response. The demonstrated predictive capability and efficiency of the analytic MCC model sets the stage for further investigations involving unidirectional metal matrix composites with functionally-graded constituents.

ACKNOWLEDGEMENTS

The authors gratefully acknowledge the support provided by the NASA-Lewis Research Center through the contract **NAS3-26571**. Special thanks go to Dr. Steven Arnold of the NASA-Lewis Research Center, the technical monitor of this contract, for his valuable suggestions and comments in the course of the preparation of this manuscript.

REFERENCES

ABAQUS User's Manual v4.8, (1989), Hibbitt, Karlsson & Sorensen, Inc., Pawtucket, R.I.

Arnold, S. M., Arya, V. K. and Melis, M. E. (1990), Elastic/Plastic Analyses of Advanced Composites Investigating the Use of the Compliant Layer Concept in Reducing Residual Stresses Resulting from Processing, *NASA Technical Memorandum 103204*, Lewis Research Center.

Arnold, S. M., Arya, V. K. and Melis, M. E. (1992), "Reduction of Thermal Residual Stresses in Advanced Metallic Composites Based upon a Compensating/Compliant Layer Concept," *J. Composite Materials*, **26**, (9), 1287.

Arnold, S. M. and Wilt, T. E. (1992), Influence of Engineered Interfaces on Residual Stresses and Mechanical Response in Metal Matrix Composites, *NASA Technical Memorandum 105438*, Lewis Research Center.

Barkalow, R. H., Hecht, R. J. and Shamakian, R. L. (1985), "Advanced Coating R & D," *AFWAL-TR-83-4086*, Pratt & Whitney.

Benveniste, Y., Dvorak, G. J., and Chen, T. (1991), On the Effective Properties of Composites with Coated Cylindrically Orthotropic Fibers, *Mechanics of Materials*, **12**, 289.

Bowman, R. (1992), Private communication. Materials Division, NASA Lewis Research Center, Cleveland, OH.

Bufler, H. (1971), Theory of Elasticity of a Multilayered Media, *J. Elasticity*, **1**, 125.

Christensen, R. M. and Lo, K. H. (1979), Solutions for Effective Shear Properties in Three Phase Sphere and Cylinder Models, *J. Mech. Phys. Solids*, **27** (4), 315.

Derstine, M. S. and Pindera, M-J. (1989), Nonlinear Response of Composite Tubes Under Combined Thermomechanical Loading, in *Composites and Other New Materials for PVP : Design and Analysis Considerations, ASME PVP-Vol. 174*, D. Hui, T. J. Kozik, G. E. O. Widera and M. Shiratori, Eds., 19.

Dvorak, G. J. and Rao, M. S. M. (1976a), Thermal Stresses in Heat-Treated Fibrous Composites, *J. Appl. Mech.*, **43**, 619.

Dvorak, G. J. and Rao, M. S. M. (1976b), Axisymmetric Plasticity Theory of Fibrous Composites, *Int. J. Engr. Sci.*, **14**, 361.

Dvorak, G. J. and Bahei-el-Din, Y. A. (1979), Elastic-Plastic Behavior of Fibrous Composites, *J. Mech Phys. Solids*, **27**, 51.

Hashin, Z. (1962), The Elastic Moduli of Heterogeneous Materials, *J. Appl. Mech.*, **29**, 143.

Hashin, Z. (1990), Thermoelastic Properties and Conductivity of Carbon/Carbon Fiber Composites, *Mechanics of Materials*, **8**, 293.

Hill, R., (1965), Theory of Mechanical Properties of Fibre-Strengthened Materials. II. Inelastic Behavior, *J. Mech. Phys. Solids*, **12**, 213.

Jansson, S. and Leckie, F. A. (1992), "Reduction of Thermal Stresses in Continuous Fiber Reinforced Metal Matrix Composites with Interface Layers," *J. Composite Materials*, **26**, (10), 1474.

Mendelson, A. (1983), *Plasticity: Theory and Applications*, Robert E. Krieger Publishing Company, Malabar, Fl., (reprint edition), 164.

Mulhern, J. F., Rogers, T. G., and Spencer, A. J. M., (1967) Cyclic Extension of an Elastic Fibre with an Elastic-Plastic Coating, *J. Inst. Maths. Applics.*, **3**, 21.

Pindera, M-J. (1991), Local/Global Stiffness Matrix Formulation for Composite Materials and Structures, *Composites Engineering*, **1**, (2), 69.

Pindera, M-J. and Freed, A. D. (1992), The Effect of Matrix Microstructure on the Evolution of Residual Stresses in Titanium Aluminide Composites, in *Constitutive Behavior of High-Temperature Composites, ASME MD-Vol. 40*, Eds., B. S. Majumdar, G. M. Newaz, and S. Mall, 37.

Pindera, M-J., Freed, A. D. and Arnold, S. M. (1992), "Effects of Fiber and Interfacial Layer Morphologies on the Thermoplastic Response of Metal Matrix Composites," *Int. Journal Solids and Structures*, (in press). See also: Pindera, M-J., Freed, A. D. and Arnold, S. M., "Effects of Fiber and Interfacial Layer Architectures on the Thermoplastic Response of Metal Matrix Composites," *NASA Technical Memorandum 105802*, NASA Lewis Research Center.

Sutcu, M. (1992), A Recursive Concentric Cylinder Model for Composites Containing Coated Fibers, *Int. J. Solids Structures*, **29**, 197-213.

Warwick, C. W. and Clyne, T. W. (1991), Development of Composite Coaxial Cylinder Stress Analysis Model and Its Application to SiC Monofilament Systems, *Journal of*

Materials Science, **26**, 3817.

Wawner, F. E. and Gundel, D. B. (1991), Investigation of the Reaction Kinetics Between SiC Fibers and Selectively Alloyed Titanium Matrices, *School of Engineering and Applied Science Technical Report (Grant No. NAG-1-745*, Department of Materials Science, University of Virginia, Charlottesville, VA.

Williams, T. O., Arnold, S. M., and Pindera, M-J. (1993), Effectiveness of Graded Interfacial Layers in Reducing Residual Stresses in Titanium Matrix Composites, *Proc. 1993 TMS Annual Meeting*, Denver, Colorado.

Table 1. Material properties of SCS6 SiC fiber and titanium matrix (Arnold et al. (1990)).

Material properties	75°F	392°F	797°F	1112°F	1202°F	1500°F
SiC fiber						
α (10^{-6} / °F)	1.96	2.01	2.15	2.33	2.38	2.50
E (Msi)	58.00	58.00	58.00	58.00	58.00	58.00
ν	0.25	0.25	0.25	0.25	0.25	0.25
Ti-24Al-11Nb matrix						
α (10^{-6} / °F)	5.00	5.20	5.70	5.85	5.90	6.15
E (Msi)	16.00	14.50	11.00	12.50	9.89	6.20
ν	0.26	0.26	0.26	0.26	0.26	0.26
σ_y (ksi)	53.89	59.00	53.70	42.20	39.10	24.00
H (Msi)	3.33	0.44	0.32	0.19	0.097	0.00

Note: In the table above and the tables that follow, α is the instantaneous thermal expansion coefficient; E is the Young's modulus, ν is the Poisson's ratio; σ_y is the yield stress; and H is the hardening slope based on a bilinear representation of the elastic-plastic stress-strain response.

Table 2. Material properties of Al_2O_3 fiber and NiAl (Bowman, 1992), NiCrAlY1, and NiCrAlY2 (Barkalow et al., 1985) matrices.

Properties	70°F	800°F	1200°F	1400°F	1600°F	1800°F	2000°F	2400°F
Al_2O_3 fiber								
α (10^{-6} / °F)	3.35	4.86	5.42	5.63	5.79	5.91	5.98	5.97
E (Msi)	61.10	59.83	59.60	59.33	59.07	58.80	53.13	50.30
ν	0.20	0.20	0.20	0.20	0.20	0.20	0.20	0.20
NiAl matrix								
α (10^{-6} / °F)	7.12	8.24	8.76	9.01	9.23	9.45	9.69	9.95
E (Msi)	28.00	25.59	24.27	23.61	22.95	22.29	19.29	10.14
ν	0.32	0.32	0.32	0.32	0.32	0.32	0.32	0.32
σ_y (ksi)	45.70	22.50	16.06	13.07	10.62	7.79	5.30	3.39
H (Msi)	0.50	0.50	0.50	0.50	0.50	0.50	0.50	0.50
NiCrAlY1* matrix								
α (10^{-6} / °F)	5.44	7.76	9.03	9.67	10.30	10.94	11.57	12.84
E (Msi)	27.00	25.30	21.40	17.70	12.80	7.60	3.10	0.10
ν	0.30	0.30	0.30	0.30	0.30	0.30	0.30	0.30
σ_y (ksi)	150.00	146.00	135.80	101.20	74.90	21.90	5.00	1.00
H (Msi)	0.10	0.10	0.10	0.10	0.10	0.10	0.10	0.10
NiCrAlY2** matrix								
α (10^{-6} / °F)	5.44	7.76	9.03	9.67	10.30	10.94	11.57	12.84
E (Msi)	19.50	16.80	14.70	11.60	8.90	5.20	2.10	0.10
ν	0.30	0.30	0.30	0.30	0.30	0.30	0.30	0.30
σ_y (ksi)	117.80	104.10	99.40	71.00	29.40	11.00	3.80	0.70
H (Msi)	0.10	0.10	0.10	0.10	0.10	0.10	0.10	0.10

* *NiCrAlY1 matrix chemical composition: Ni-10.2Cr-9.3Al-6.0Ta-0.22Hf-0.43Y*
** *NiCrAlY2 matrix chemical composition: Ni-17.8Cr-12.5Al-0.61Y-0.73Hf-20.8Co*

Table 3. Comparison of stresses and radial displacements generated by the present model and ABAQUS.

Radial location	σ_{xx} (psi)	$\sigma_{\theta\theta}$ (psi)	σ_{rr} (psi)	w(r) ($\times 10^{-2}$ in/in)
0.6320 (fiber)				
ABAQUS (88 el.)	-83,855	-19,579	-19,580	-0.19012
ABAQUS (296 el.)	-83,856	-19,580	-19,580	-0.19012
ABAQUS (580 el.)	-83,854	-19,579	-19,577	-0.19012
Present model	-83,840	-19,590	-19,590	-0.19010
0.6320 (r_{inner} interfacial layer)				
ABAQUS (88 el.)	38,960	41,897	-19,557	-0.19012
ABAQUS (296 el.)	38,967	41,902	-19,547	-0.19012
ABAQUS (580 el.)	38,973	41,908	-19,539	-0.19012
Present model	38,900	41,870	-19,590	-0.19010
0.6952 (r_{outer} interfacial layer)				
ABAQUS (88 el.)	41,792	39,235	-14,085	-0.41143
ABAQUS (296 el.)	41,743	39,190	-14,141	-0.41145
ABAQUS (580 el.)	41,813	39,255	-14,056	-0.41141
Present model	41,720	39,200	-14,130	-0.41150
0.6952 (matrix)				
ABAQUS (88 el.)	50,627	36,758	-13,831	-0.41143
ABAQUS (296 el.)	50,507	36,447	-14,053	-0.41145
ABAQUS (580 el.)	50,445	36,541	-14,087	-0.41141
Present model	50,320	36,640	-14,130	-0.41150
1.0 (matrix)				
ABAQUS (88 el.)	62,783	28,045	97	-0.72439
ABAQUS (296 el.)	62,778	28,038	94	-0.72439
ABAQUS (580 el.)	62,714	28,004	14	-0.72439
Present model	62,700	27,990	0	-0.72450

Table 4. Comparison of CPU times between the present model and ABAQUS for cooling down of a SiC/Ti_3Al unidirectional composite from 1500°F to 75°F.

	CPU time (seconds)
1 interfacial layer	
Present model (189 integration stations)	12.76
ABAQUS (88-element mesh)	87.24
ABAQUS (296-element mesh)	237.57
ABAQUS (580-element mesh)	511.00
3 interfacial layers	
Present model (189 integration stations)	12.76
ABAQUS (708-element mesh)	714.41

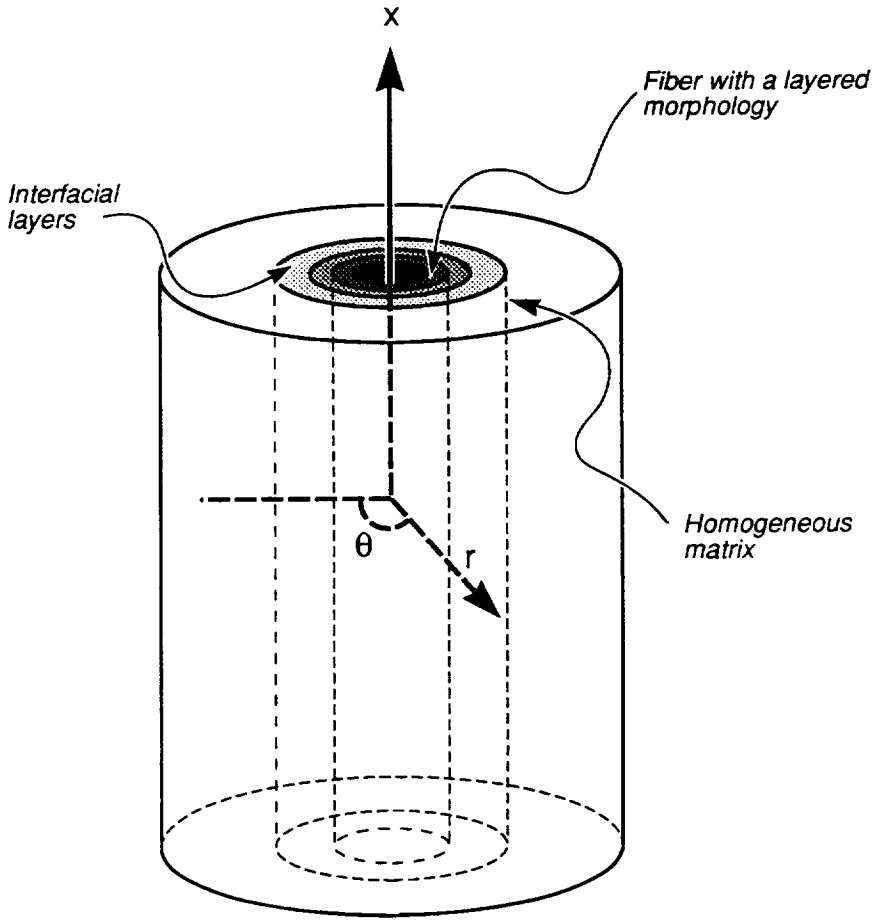

Figure 1 - Multiple concentric cylinder model.

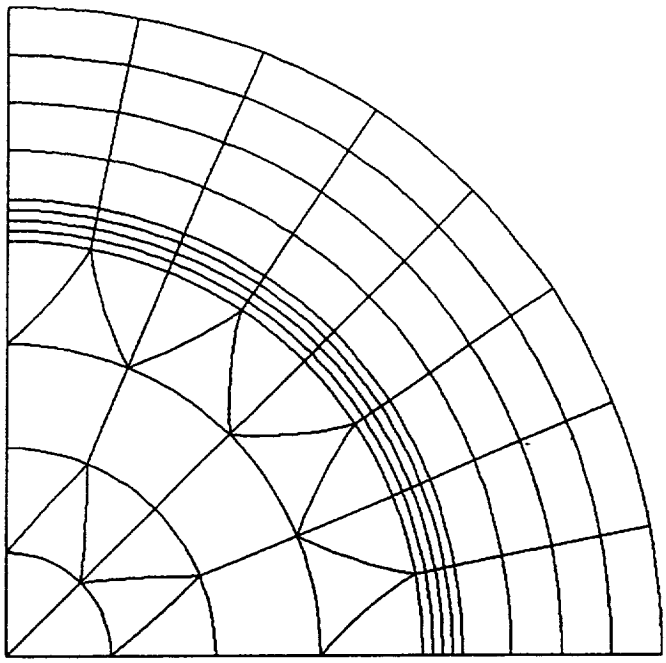

A.) 88 Element Mesh

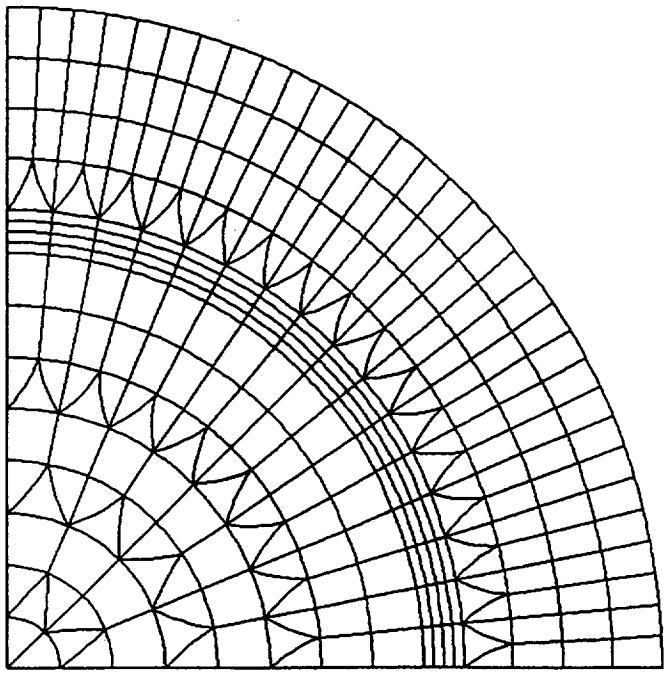

B.) 296 Element Mesh

Figure 2 - Finite-element mesh configurations for a concentric cylinder with one interfacial layer: a.) 88 element mesh; b.) 296 element mesh; c.) 580 element mesh.

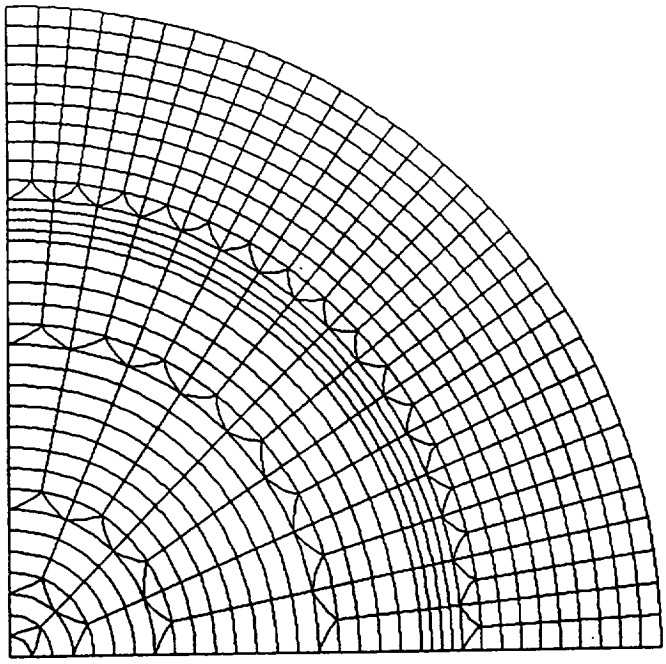

C.) 580 Element Mesh

Figure 2 - Concluded.

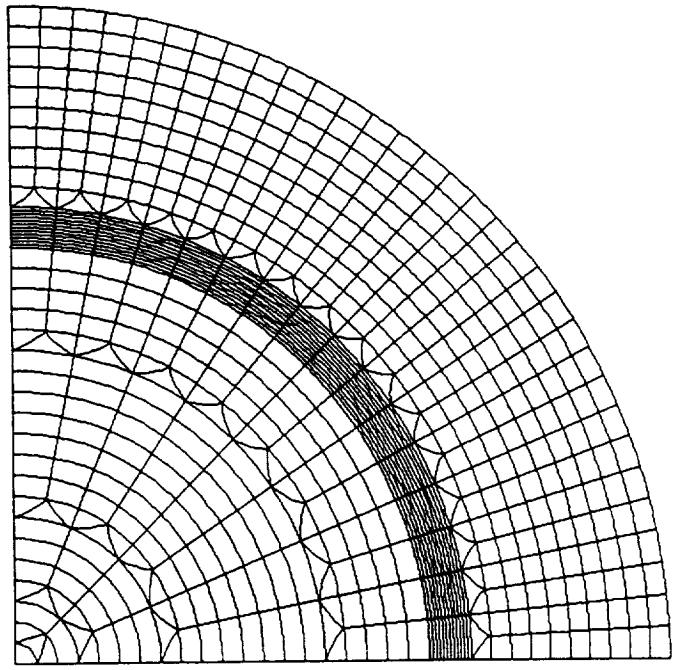

Figure 3 - Finite-element mesh configuration with 708 elements for a concentric cylinder with three interfacial layers.

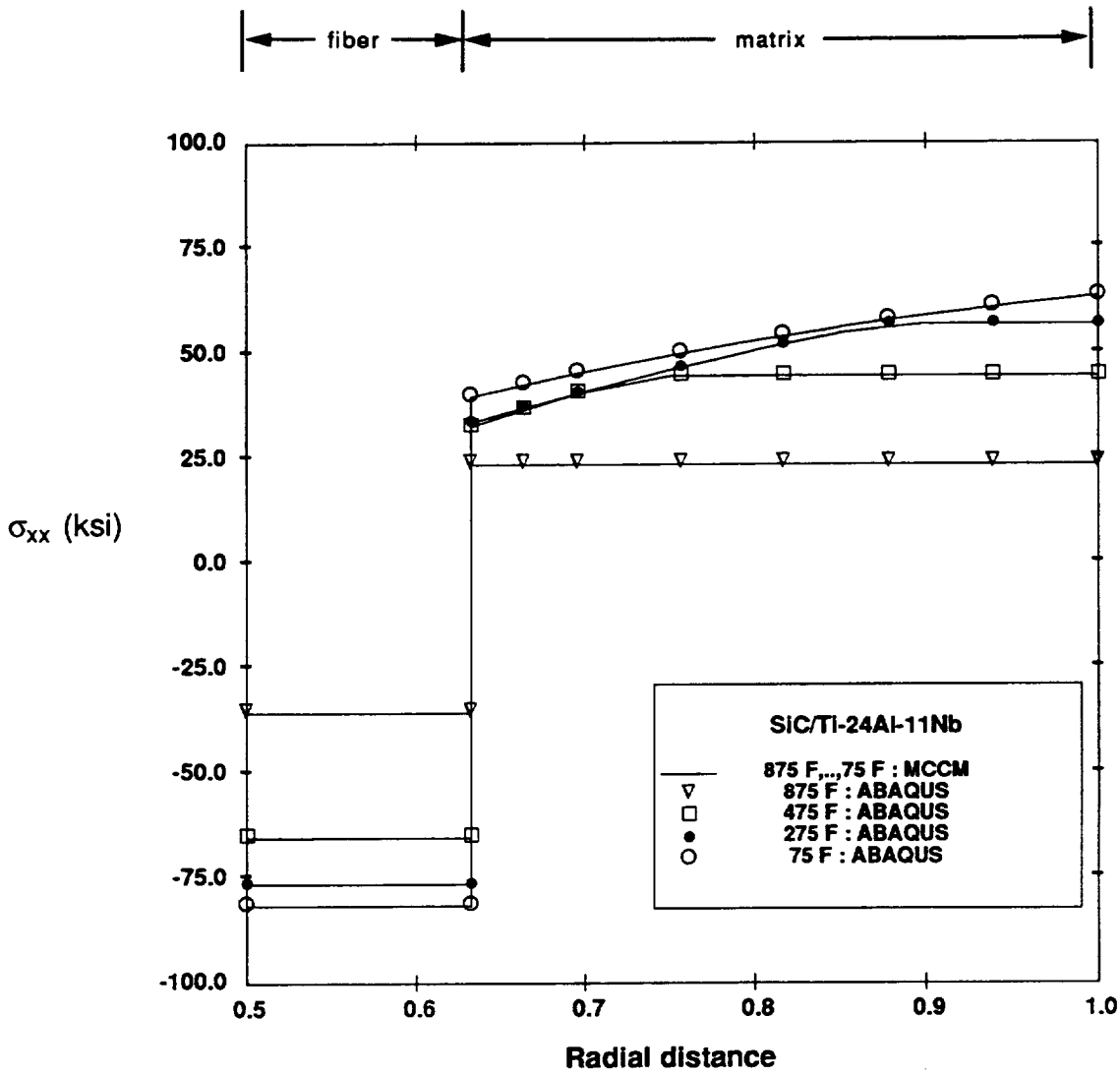

A.)

Figure 4 - Comparison between finite-element and present solution stress distributions in a SiC/Ti-24Al-11Nb composite without an interface at T = 875°F, 475°F, 275°F and 75°F after cool down from 1500°F: a.) axial stress; b.) hoop stress; c.) radial stress.

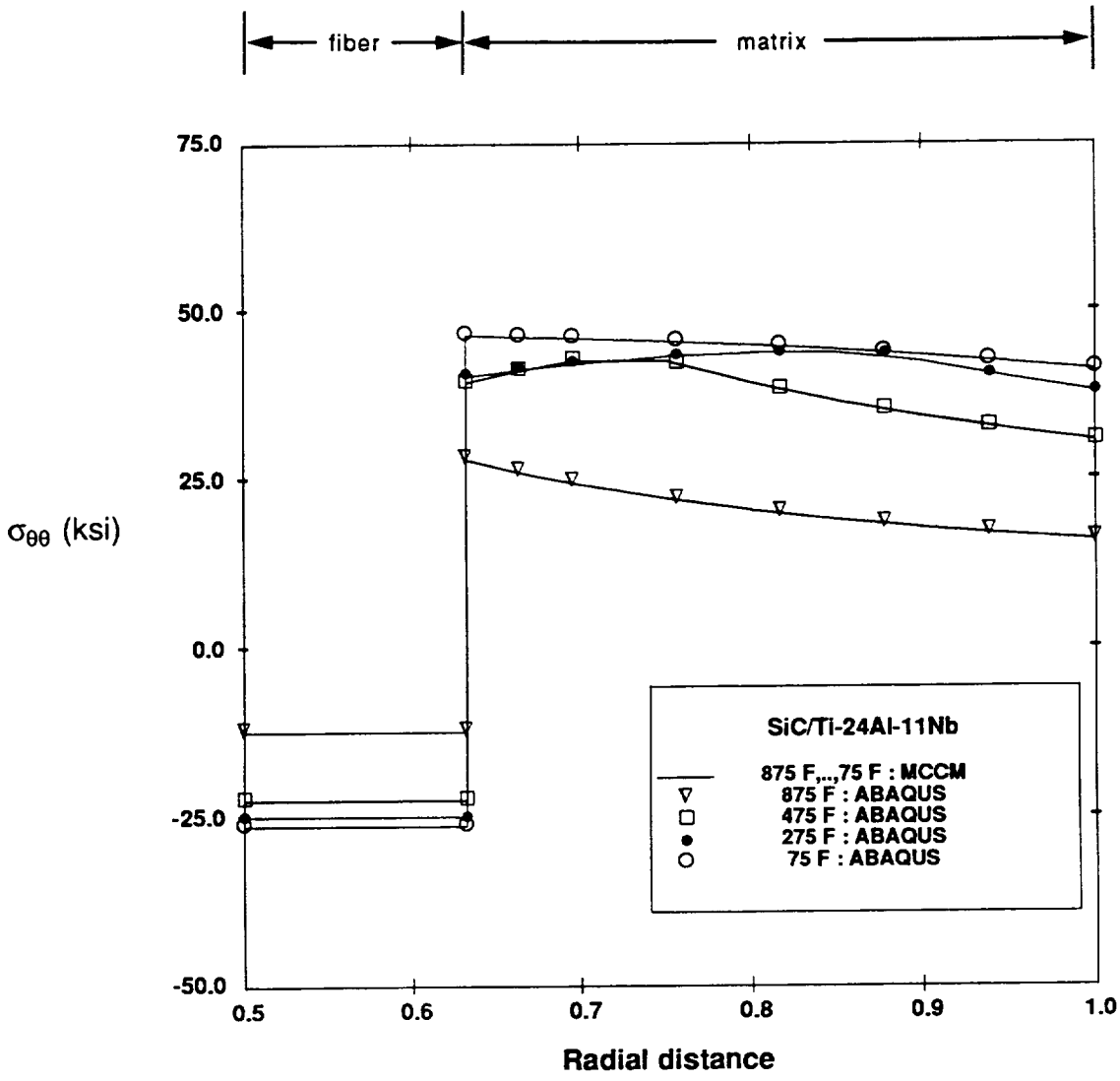

B.)

Figure 4 - Continued.

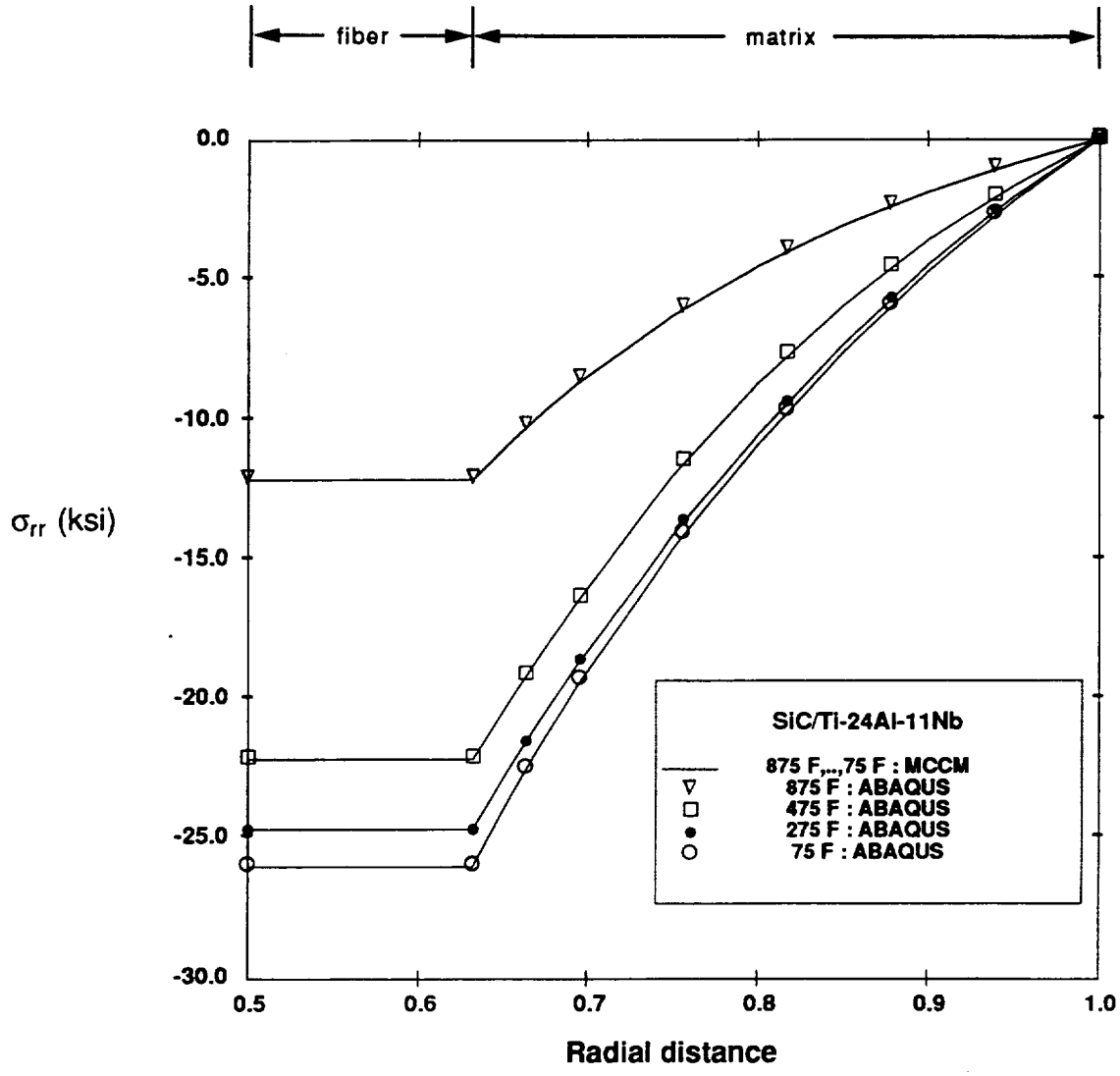

C.)

Figure 4 - Concluded.

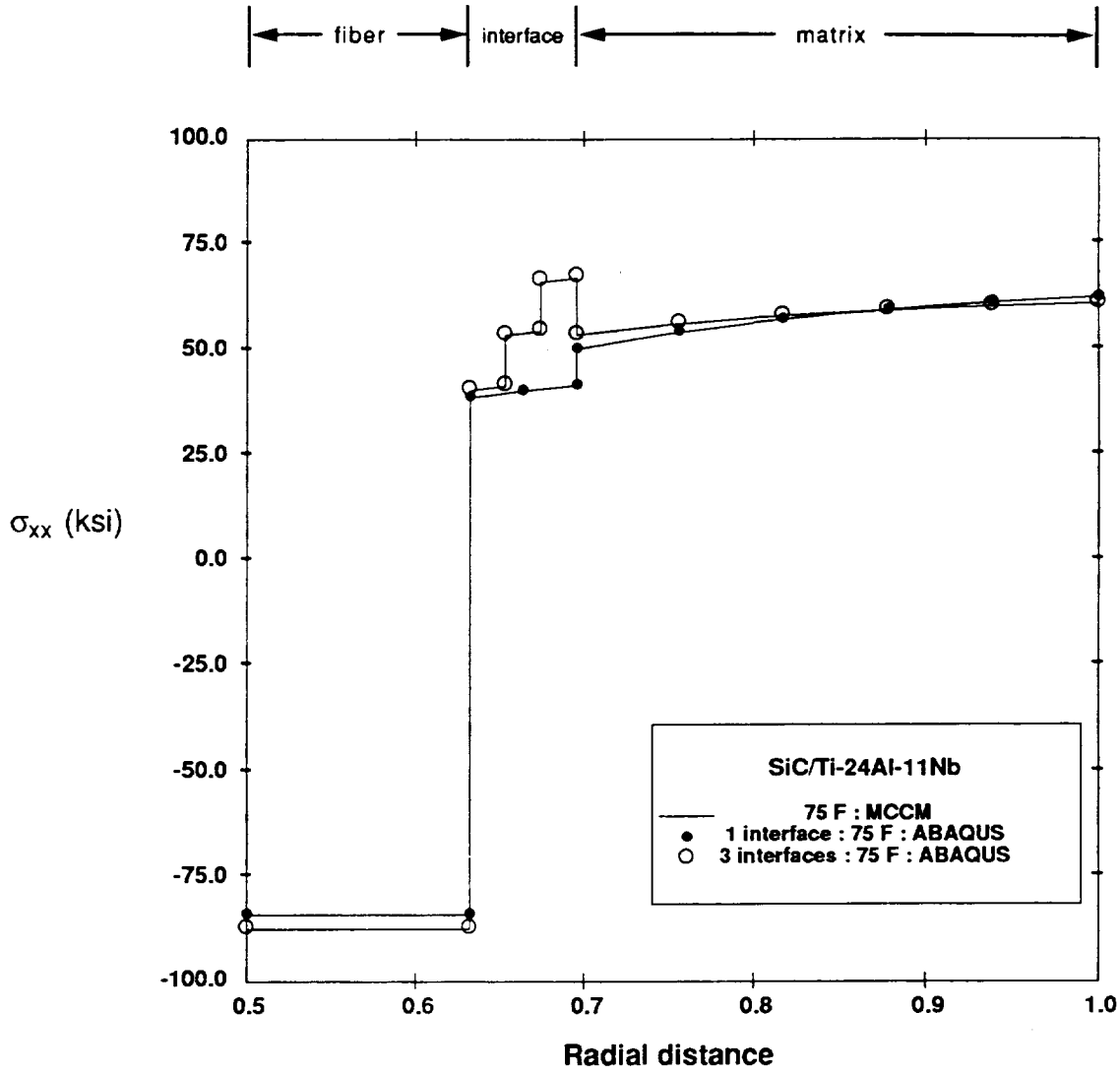

A.)

Figure 5 - Comparison between finite-element and present solution stress distributions in a SiC/Ti-24Al-11Nb composite with an one-layer and three-layer interface at T = 75°F after cool down from 1500°F: a.) axial stress; b.) hoop stress; c.) radial stress.

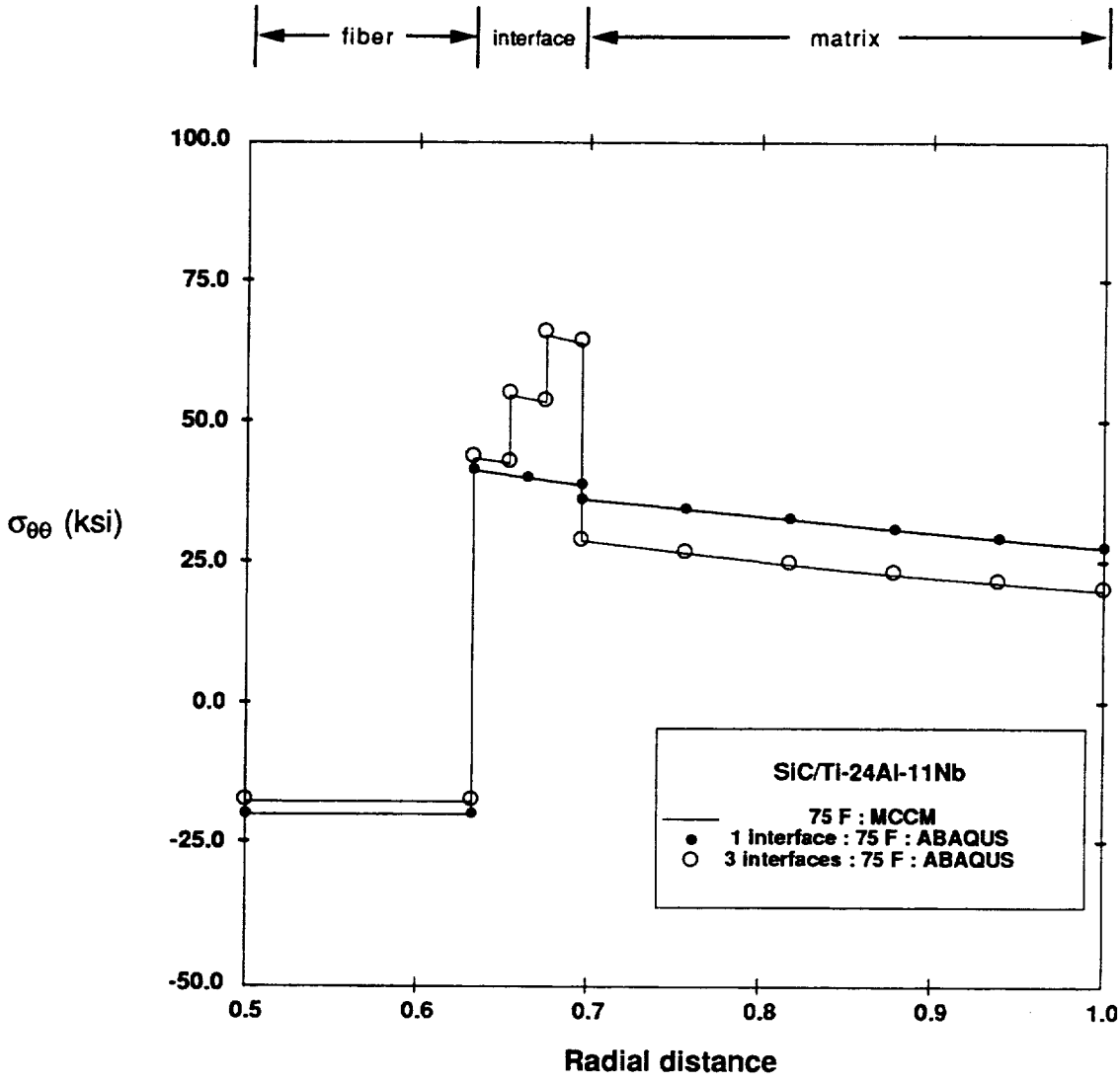

B.)

Figure 5 - Continued.

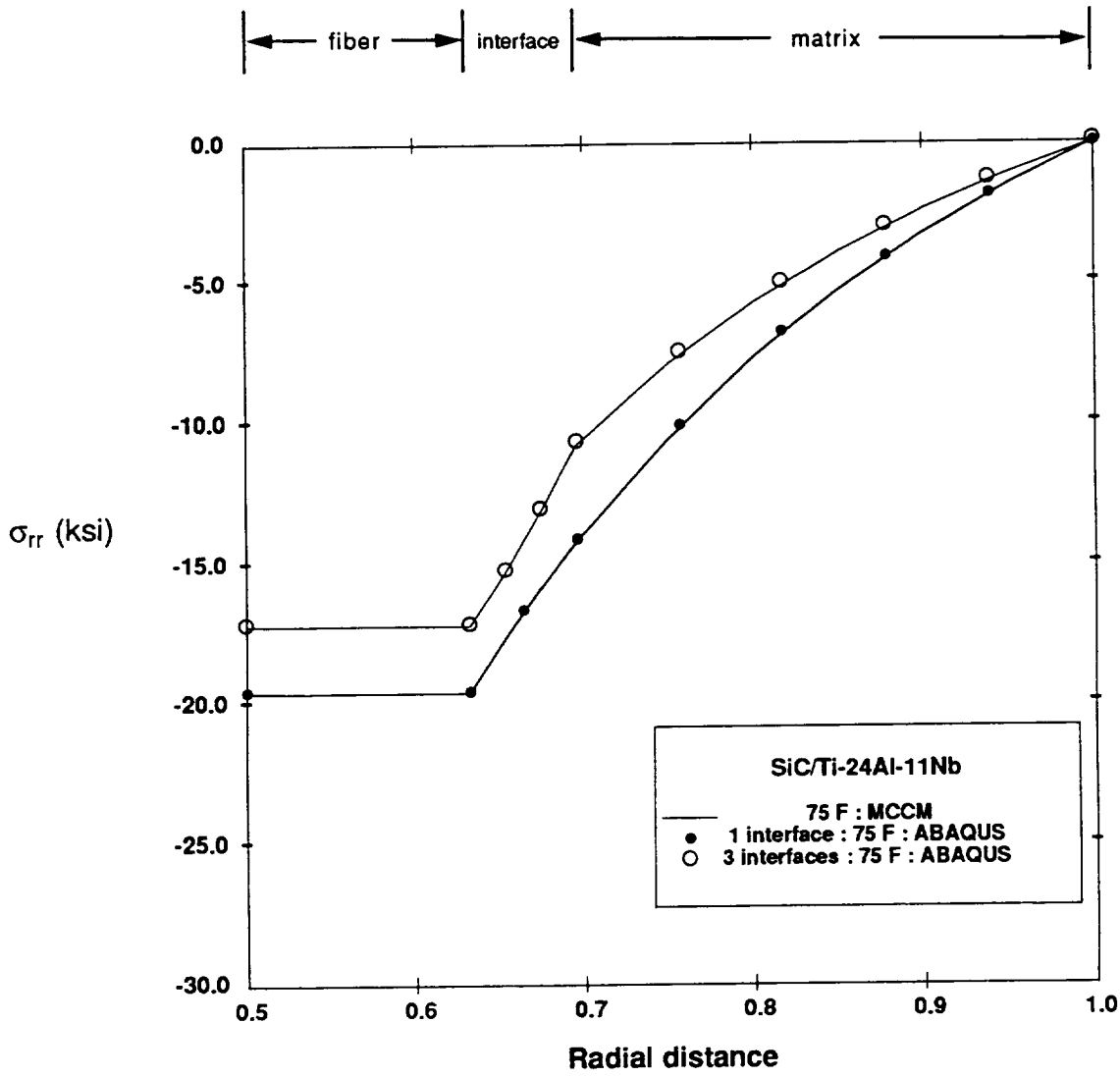

C.)

Figure 5 - Concluded.

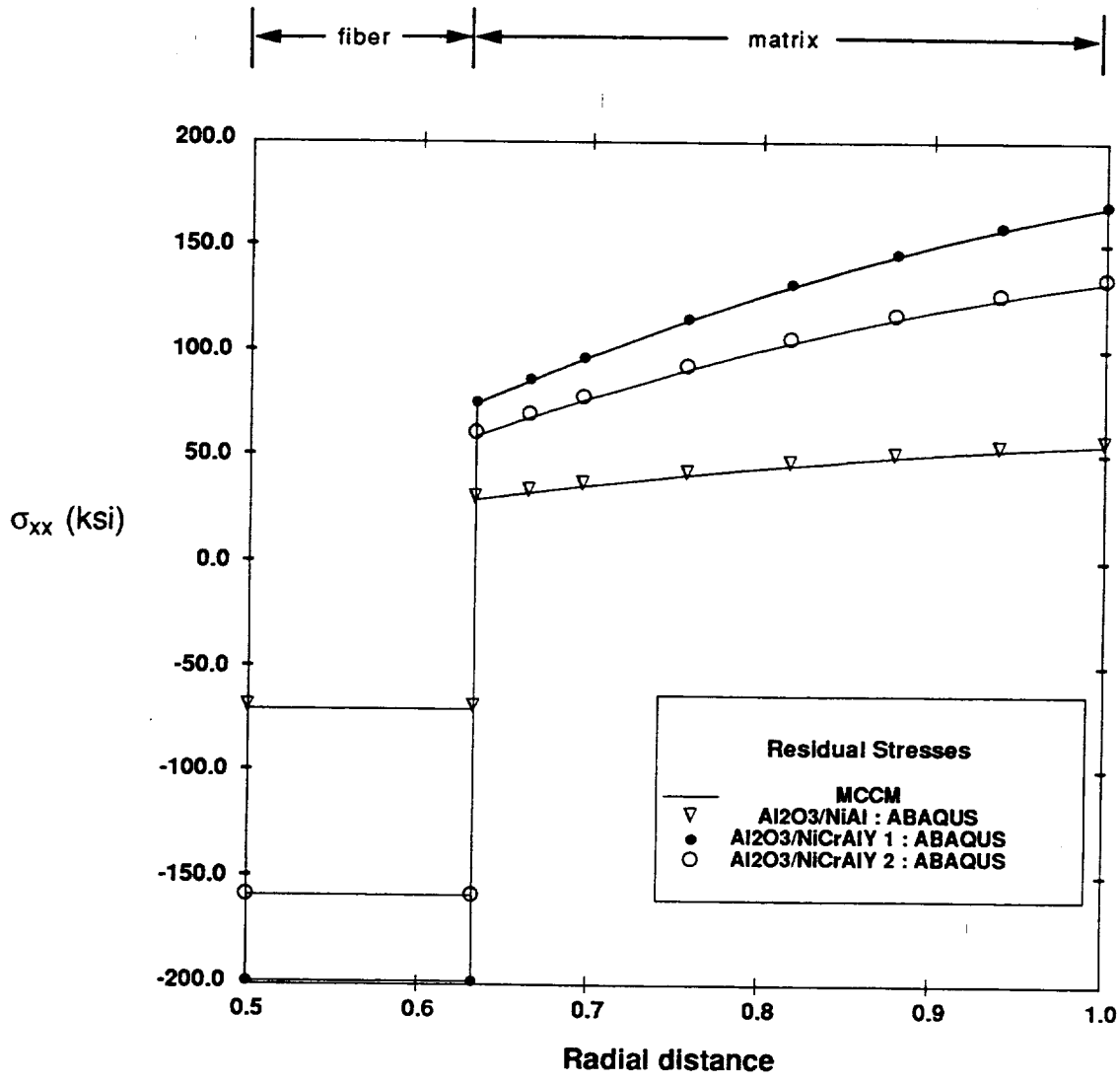

A.)

Figure 6 - Comparison between finite-element and present solution stress distributions in a Al_2O_3/NiAl, Al_2O_3/NiCrAlY1 and Al_2O_3/NiCrAlY2 composite without an interface at T = 70°F after cool down from 2300°F: a.) axial stress; b.) hoop stress; c.) radial stress.

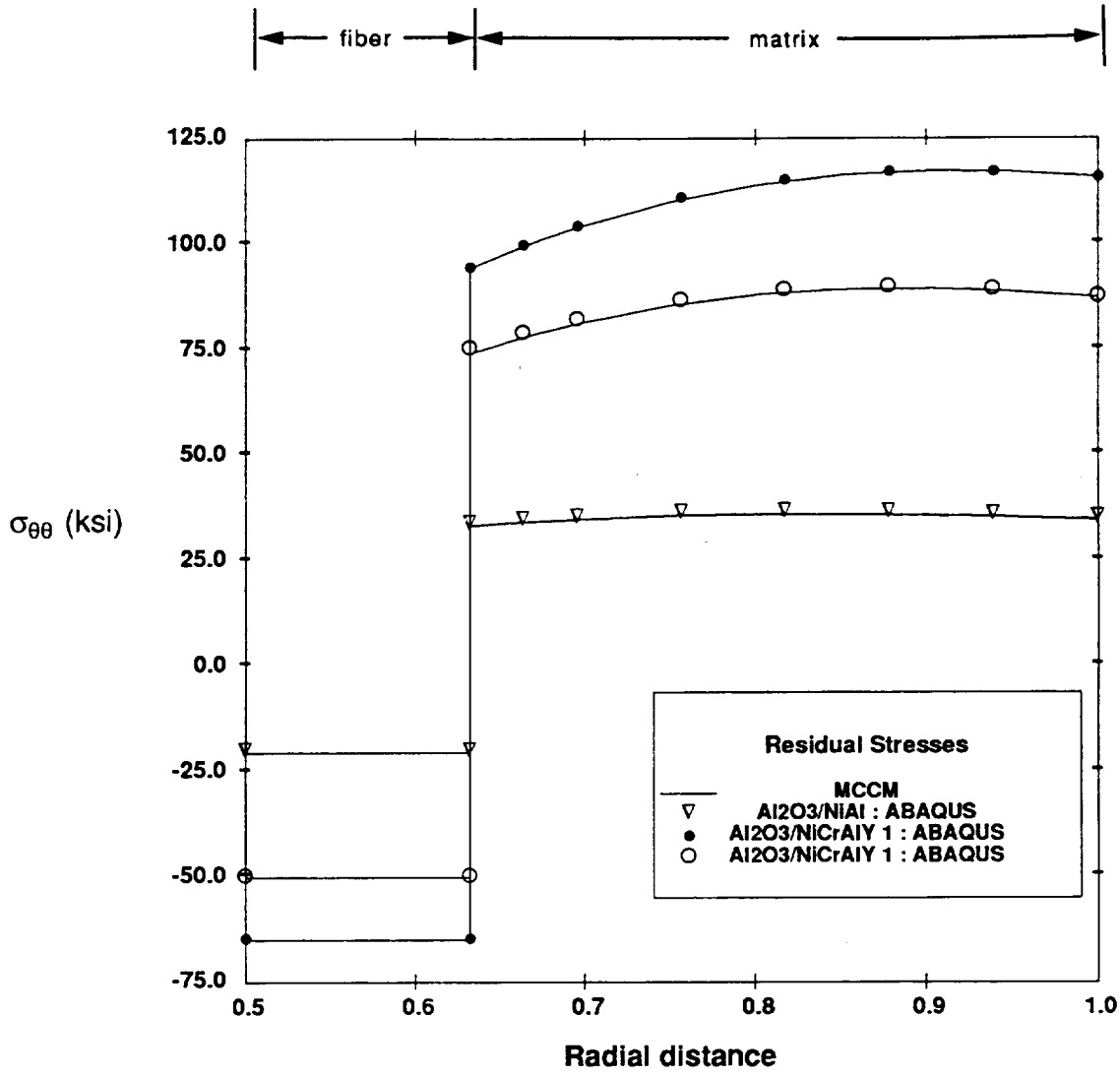

B.)

Figure 6 - Continued.

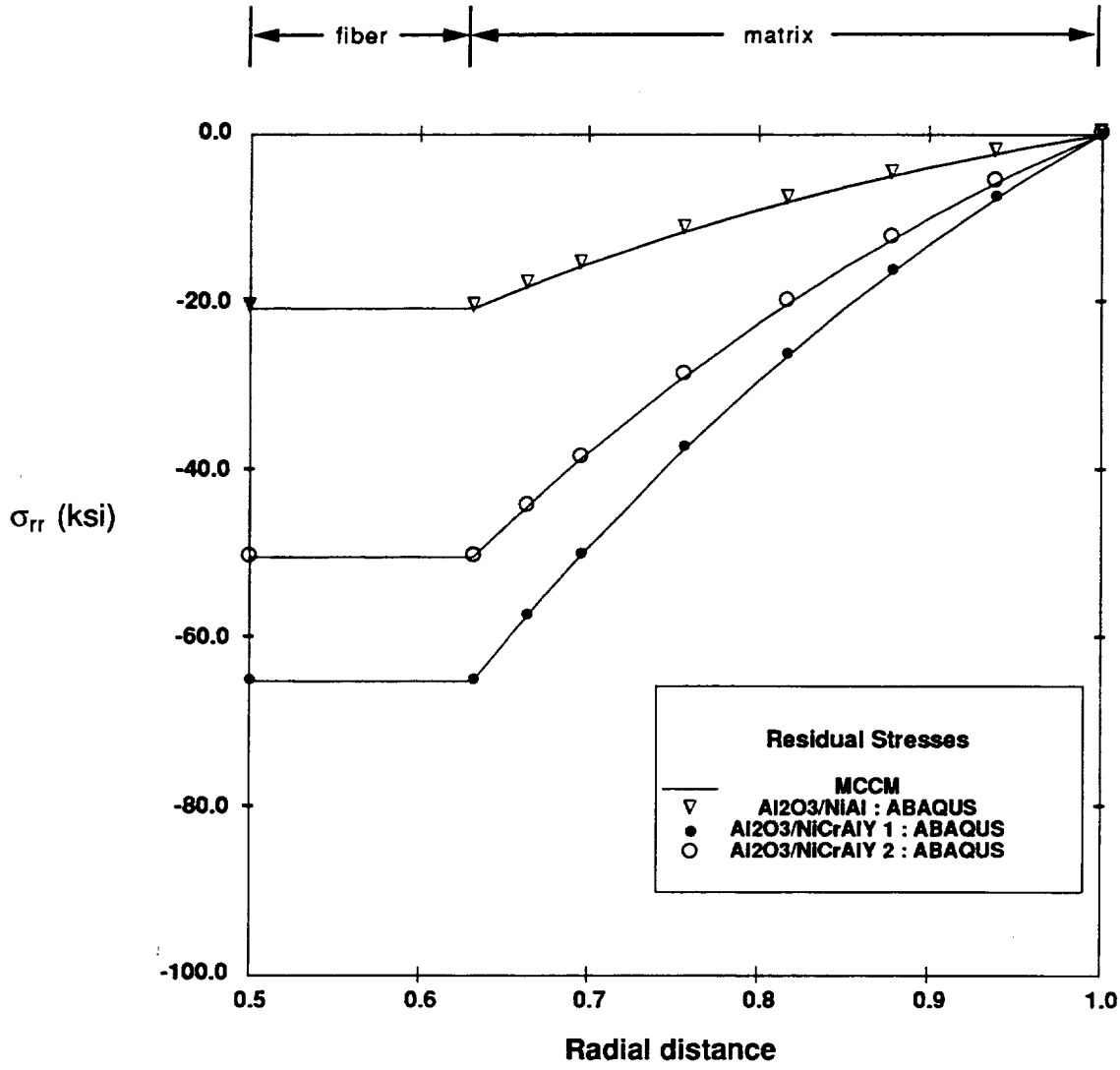

C.)

Figure 6 - Concluded.

REPORT DOCUMENTATION PAGE

Form Approved
OMB No. 0704-0188

Public reporting burden for this collection of information is estimated to average 1 hour per response, including the time for reviewing instructions, searching existing data sources, gathering and maintaining the data needed, and completing and reviewing the collection of information. Send comments regarding this burden estimate or any other aspect of this collection of information, including suggestions for reducing this burden, to Washington Headquarters Services, Directorate for Information Operations and Reports, 1215 Jefferson Davis Highway, Suite 1204, Arlington, VA 22202-4302, and to the Office of Management and Budget, Paperwork Reduction Project (0704-0188), Washington, DC 20503.

1. AGENCY USE ONLY (*Leave blank*)	2. REPORT DATE	3. REPORT TYPE AND DATES COVERED
	May 1993	Final Contractor Report

4. TITLE AND SUBTITLE

An Analytical/Numerical Correlation Study of the Multiple Concentric Cylinder Model for the Thermoplastic Response of Metal Matrix Composites

5. FUNDING NUMBERS

WU–510–01–50
C–NAS3–26571

6. AUTHOR(S)

Marek-Jerzy Pindera, Robert S. Salzar, and Todd O. Williams

7. PERFORMING ORGANIZATION NAME(S) AND ADDRESS(ES)

University of Virginia
Charlottesville, Virginia 22903

8. PERFORMING ORGANIZATION REPORT NUMBER

E–7856

9. SPONSORING/MONITORING AGENCY NAME(S) AND ADDRESS(ES)

National Aeronautics and Space Administration
Lewis Research Center
Cleveland, Ohio 44135–3191

10. SPONSORING/MONITORING AGENCY REPORT NUMBER

NASA CR–191142

11. SUPPLEMENTARY NOTES

Project Manager, Steven M. Arnold, Structures Division, (216) 433–3334.

12a. DISTRIBUTION/AVAILABILITY STATEMENT

Unclassified - Unlimited
Subject Categories 24 and 49

12b. DISTRIBUTION CODE

13. ABSTRACT (*Maximum 200 words*)

The utility of a recently developed analytical micromechanics model for the response of metal matrix composites under thermal loading is illustrated by comparison with the results generated using the finite-element approach. The model is based on the concentric cylinder assemblage consisting of an arbitrary number of elastic or elastoplastic sublayers with isotropic or orthotropic, temperature-dependent properties. The elastoplastic boundary-value problem of an arbitrarily layered concentric cylinder is solved using the local/global stiffness matrix formulation (originally developed for elastic layered media) and Mendelson's iterative technique of successive elastic solutions. These features of the model facilitate efficient investigation of the effects of various microstructural details, such as functionally graded architectures of interfacial layers, on the evolution of residual stresses during cool down. The available closed-form expressions for the field variables can readily be incorporated into an optimization algorithm in order to efficiently identify optimal configurations of graded interfaces for given applications. Comparison of residual stress distributions after cool down generated using finite-element analysis and the present micromechanics model for four composite systems with substantially different temperature-dependent elastic, plastic and thermal properties illustrates the efficacy of the developed analytical scheme.

14. SUBJECT TERMS

Thermal residual stresses; Elastic plastic; Metal matrix composites; Micromechanics; Concentric cylinder; Optimization

15. NUMBER OF PAGES

34

16. PRICE CODE

A03

17. SECURITY CLASSIFICATION OF REPORT	18. SECURITY CLASSIFICATION OF THIS PAGE	19. SECURITY CLASSIFICATION OF ABSTRACT	20. LIMITATION OF ABSTRACT
Unclassified	Unclassified	Unclassified	

National Aeronautics and
Space Administration

Lewis Research Center
Cleveland, Ohio 44135

Official Business
Penalty for Private Use $300

FOURTH CLASS MAIL

ADDRESS CORRECTION REQUESTED